

A simple and efficient all-optical production of spinor condensates

J. Jiang,¹ L. Zhao,¹ M. Webb,¹ N. Jiang,² H. Yang,² and Y. Liu^{1,*}

¹*Department of Physics, Oklahoma State University, Stillwater, OK 74078*

²*Center for Quantum Information, IIIS, Tsinghua University, Beijing, China*

(Dated: February 8, 2022)

We present a simple and optimal experimental scheme for an all-optical production of a sodium spinor Bose-Einstein condensate (BEC). With this scheme, we demonstrate that the number of atoms in a pure BEC can be greatly boosted by a factor of 5 in a simple setup that includes a single-beam optical trap or a crossed optical trap. This optimal scheme avoids technical challenges associated with some all-optical BEC methods, and can be applied to other optically trappable atomic species. In addition, we find a good agreement between our theoretical model and data. The upper limit for the efficiency of evaporative cooling in all-optical BEC approaches is also discussed.

PACS numbers: 64.70.fm, 37.10.Jk, 32.60.+i, 67.85.Hj

In the last two decades, many techniques have been developed to reliably generate a BEC of more than 10^4 atoms. Almost every one of these techniques requires evaporative cooling in a trapping potential, including a magnetic trap, an optical dipole trap (ODT), or a combined magnetic and optical potential [1–5]. Among these techniques, all-optical methods have been proven to be versatile and popularly applied in producing quantum degenerate gases of both bosonic [6–14] and fermionic [15] species. ODTs have tight confinement which allows for fast evaporation with a duty cycle of a few seconds [6]. Unlike magnetic potentials that only trap atoms in the weak-field seeking spin state, an ODT can confine all spin components. This is crucial for creating vector (spinor) BECs with a spin degree of freedom [16]. ODTs can also be applied to a wider variety of atomic species (e.g., Ytterbium, alkaline earth metals, and Cesium) which cannot be feasibly condensed in a magnetic trap [8, 13]. In addition, optical trapping does not require magnetic coils around trapped atoms, which not only provides better optical access but also yields less residual magnetic fields. The simplicity and versatility of ODTs widens the accessibility of BEC research on many-body physics, precision measurements, and quantum information science [18].

Forced evaporation in an ODT can be performed by simply reducing its trap depth U (e.g., lowering the trapping laser power). In this process, collision rates decrease with U , which leads to slow rethermalization and eventually stagnation in evaporative cooling. Several methods have been reported to overcome this difficulty, including tilting an ODT with a magnetic field gradient [17], using a misaligned crossed ODT [12, 14], compressing an ODT with a mobile lens [11], or applying multiple ODTs for staged evaporation [8, 10]. In this paper, however, we show that these methods may not be necessary. Good agreements between our model and experimental data enable us to develop an optimal ODT ramp and evaporation sequence for an all-optical production of sodium

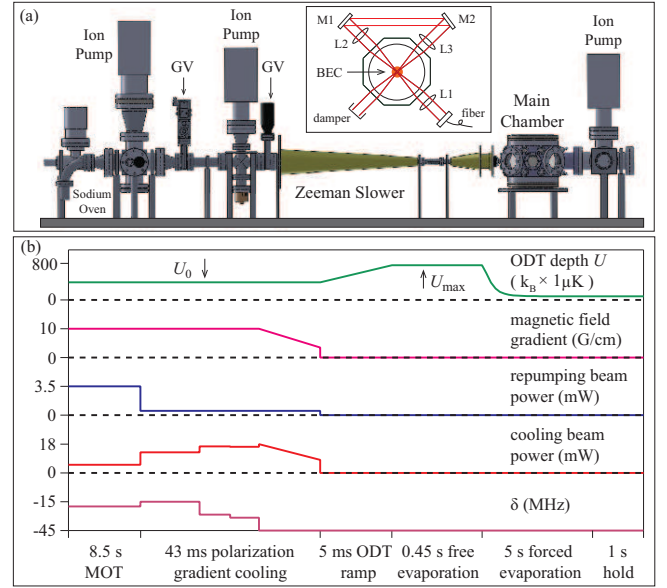


FIG. 1. (color online) (a). Schematic of our apparatus. GV stands for a pneumatic gate valve. Inset: schematic of the crossed ODT setup around the main chamber. L_1 , L_2 , and L_3 are convex lenses. M_1 and M_2 are mirrors. (b). Experimental sequence of creating sodium BECs with the all-optical approach (see text). Each MOT cooling beam is detuned by δ from the cycling transition. All axes are not to scale.

BECs. With this sequence, we find that the number of atoms in a pure BEC is greatly boosted and evaporation efficiency $\gamma = -d(\ln D)/d(\ln N)$ can be 3.5 in a simple setup that includes a single-beam ODT or a crossed ODT. Here D is the phase space density and N is the atom number. We also show an upper limit for γ at a given truncation parameter $\eta = U/k_B T$, and demonstrate that a constant η does not yield more efficient evaporative cooling. Here T is the atom temperature and k_B is the Boltzmann constant. This optimal experimental scheme allows us to avoid technical challenges associated with some all-optical BEC approaches.

Figure 1(a) shows a schematic of our apparatus, which

* yingmei.liu@okstate.edu

is divided via differential pumping tubes and gate valves into an atomic oven chamber, an intermediate chamber, and a main chamber where a magneto-optical trap (MOT) is located. The intermediate chamber allows us to refill alkali metals and get ultra-high vacuum (UHV) pressures back to the 10^{-12} Torr range within 24 hours. A typical experimental sequence of our all-optical BEC approach is shown in Fig. 1(b). Hot atoms are slowed down by a spin-flip Zeeman slower as elaborated in Ref. [19]. The slowed atoms are collected in a standard MOT which is constructed with six cooling beams and a pair of 24-turn anti-Helmholtz coils. Each MOT cooling beam is detuned by $\delta = -20$ MHz from the cycling transition, has a power of 6 mW, and combines with one 3.5 mW MOT repumping beam in a single-mode fiber. After 8.5 s of MOT loading, a three-step polarization gradient cooling process efficiently cools 3×10^8 atoms to 40 μ K [20]. To depump atoms into the F=1 hyperfine states, the repumping beams are extinguished 1 ms before cooling beams and MOT coils are turned off.

A crossed ODT consists of two far-detuned beams which originate from an infrared (IR) laser at 1064 nm and have a $1/e^2$ waist of 33 μ m at their intersection point, as shown in Fig. 1(a). A single-mode polarization-maintaining fiber is used to polish the beam mode, and to minimize pointing fluctuations due to imperfections of the IR laser and thermal contractions of an acoustic-optical modulator. As a result, atoms which are transferred from the MOT into the tightly-focused crossed ODT demonstrate a long lifetime of 8 s and a large collision rate. These are essential for all-optical BEC approaches.

We compare the efficiency of transferring laser-cooled atoms to the crossed ODT, when different experimental sequences are applied to ramp up the ODT's trap depth. Our data in Fig. 2 clearly shows that an optimal ODT ramp sequence can increase the number of atoms loaded into the crossed ODT by a factor of 2.5. This optimal ramp sequence is the best scenario of our first ODT ramp sequence. As shown in Fig. 1(b), the ODT in the first ODT ramp sequence is kept at a small trap depth U_0 during the entire laser cooling process and then linearly ramped to U_{\max} in $t_{\text{ramp}} = 5$ ms. $U_{\max} \approx k_B \times 800 \mu\text{K}$ is the maximal trap depth used in this work and $0 \leq U_0 \leq U_{\max}$. This optimal ramp sequence is a trade-off between two competing effects induced by the enormous ODT potential. If the ODT beams do not interact with the MOT, a larger U enables more atoms to be transferred to the ODT. The number of atoms loaded in the ODT is $N_{\text{ramp2}} \sim \int_0^U \rho(\epsilon) f(\epsilon) d\epsilon$, where $\rho(\epsilon)$ and $f(\epsilon)$ are the density of states and occupation number at energy ϵ , respectively. This is confirmed by our data (closed blue triangles in Fig. 2) taken with the second ODT ramp sequence, in which the ODT is linearly ramped in 5 ms from 0 to U_0 immediately after MOT beams are switched off. On the other hand, if intense ODT beams and MOT beams are turned on simultaneously, atoms experience non-negligible AC Stark

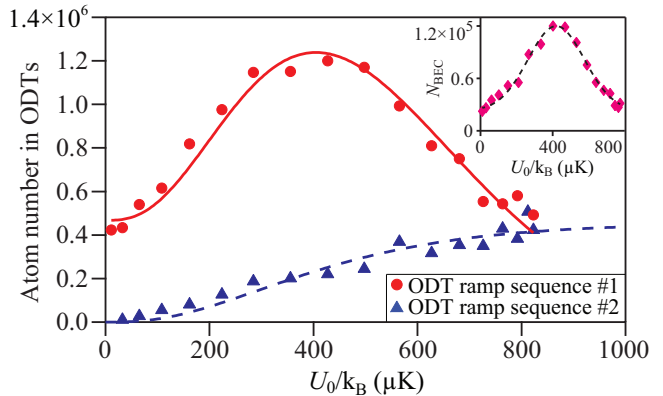


FIG. 2. (color online) The number of atoms transferred to the crossed ODT as a function of U_0 from two ODT ramp sequences. Our optimal ramp sequence is the best scenario of the first ODT ramp sequence with $U_0 \simeq U_{\max}/2$. The solid (red) line and the dashed (blue) line are fits based on N_{ramp1} and N_{ramp2} , respectively (see text). Inset: the number of atoms in a BEC as a function of U_0 , when the first ODT ramp sequence and a same evaporation curve are applied. The dashed (black) line is a Gaussian fit to data.

shifts in regions where the ODT beams and the MOT overlap. As a result, the MOT's cooling capability is impaired in the MOT and ODT overlapping regions, and the number of atoms loaded into the ODT decreases when the ODT becomes too deep. N is thus not a monotonic function of U , which is the case for our first ODT ramp sequence. The number of atoms loaded into the ODT in the first ramp sequence may be expressed as $N_{\text{ramp1}} \sim A \xi_{\text{AC}}(U_0) \int_0^{U_0} \rho(\epsilon) f(\epsilon) d\epsilon + \int_{U_0}^{U_{\max}} \rho(\epsilon) f(\epsilon) d\epsilon$. Here $\xi_{\text{AC}}(U_0) = \exp(-(\delta_{\text{AC}}(U_0))^2/\omega_0^2)$ is a correction factor due to the induced AC Stark shift $\delta_{\text{AC}}(U_0)$, while A and ω_0 are fitting parameters. Our data (closed red circles in Fig. 2) collected with the first ODT ramp sequence can be well fit by this model. The fit value of ω_0 is 1.2Γ , where $\Gamma/2\pi = 9.7$ MHz is the natural linewidth of sodium. The number of atoms in the ODT reaches its peak when the optimal ramp sequence with $U_0 \simeq U_{\max}/2$ is applied. Compared to the second ODT ramp sequence, the optimal ramp sequence allows us to use ODT beams with smaller waists while loading the same amount of laser-cooled atoms to the ODT. The resulted high initial atomic density and high collision rates from the optimal ramp sequence enable very efficient evaporative cooling. This greatly boosts the number of atoms in a BEC by a factor of 5 and a good evaporation efficiency $\gamma = 3.5$ is achieved, as shown in the inset of Fig. 2.

To optimize γ , it is necessary to understand the time evolution of the system energy E and the atom number N during an evaporation process. Similar to Ref. [14, 21–23], we use $\kappa k_B T \approx (\eta - 5)/(\eta - 4) k_B T$ to represent the average kinetic energy taken by an atom when it is removed from the ODT, and assume the mean kinetic energy and mean potential energy to be $E/2$ when η is

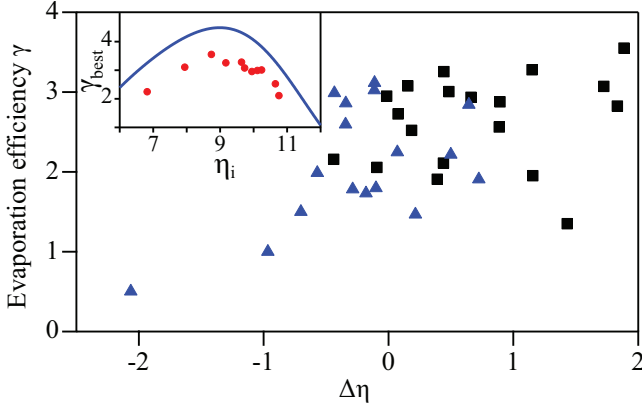


FIG. 3. (color online) Evaporation efficiency γ in 36 different evaporation processes as a function of $\Delta\eta$. Closed (black) squares are data taken with the forced evaporation time longer than 1 s. Inset: γ_{best} as a function of η_i extracted from the main figure. The solid line sets an upper limit for γ based on Eq. (4) by assuming $k_1 = k_s = 0$ (see text).

large. The time evolution of E and N is thus given by,

$$\begin{aligned}\dot{E} &= -\frac{2(\eta-4)e^{-\eta}N}{\tau_2}(U + \kappa k_B T) + \frac{\dot{U}}{U} \frac{E}{2} + \dot{E}|_{\text{loss}}, \\ \dot{N} &= -2(\eta-4)e^{-\eta}N/\tau_2 + \dot{N}|_{\text{loss}},\end{aligned}\quad (1)$$

where τ_2 is the time constant of the two-body elastic collision. In Eq. 1, $\dot{E}|_{\text{loss}}$ and $\dot{N}|_{\text{loss}}$ are due to various inelastic loss mechanisms and may be expressed as,

$$\begin{aligned}\dot{E}|_{\text{loss}} &= k_s N - k_1 N(3k_B T) - k_3 n^2 N(2k_B T), \\ \dot{N}|_{\text{loss}} &= -k_1 N - k_3 n^2 N,\end{aligned}\quad (2)$$

where k_1 and k_3 are one-body and three-body loss rates, respectively. k_s represents heating introduced by ODT beams via a number of different mechanisms, such as pointing fluctuations of the ODT beams, bad laser beam mode, and spontaneous light scattering. The term $2k_B T$ in Eq. (2) accounts for the fact that atoms in the ODT's center have higher density and thus are more affected by the three-body inelastic loss [12].

In our apparatus with the UHV pressure in the 10^{-12} Torr range, background collisions are negligible. Since the ODT beams are delivered via a single-mode polarization maintaining fiber, heating induced by the ODT beams is minimized. k_1 and k_s are thus very small. If we ignore k_1 and k_s , Eq. (1) can be simplified to

$$\dot{E} = \dot{N}\eta_{\text{eff}}k_B T + \frac{\dot{U}}{U} \frac{E}{2}, \quad (3)$$

where $\eta_{\text{eff}} = \eta + \kappa - R(\eta + \kappa - 2)$. We define $R = (\dot{N}|_{\text{loss}})/\dot{N} = 1/(1 + 2(\eta - 4)e^{-\eta}R_{\text{gTb}})$ to represent the portion of atom losses due to inelastic collisions, where R_{gTb} is the ratio of inelastic collision time constant to τ_2 . From solving the above equations, γ may be expressed as,

$$\gamma = \eta_{\text{eff}} - 4 = \eta + \kappa - R(\eta + \kappa - 2) - 4, \quad (4)$$

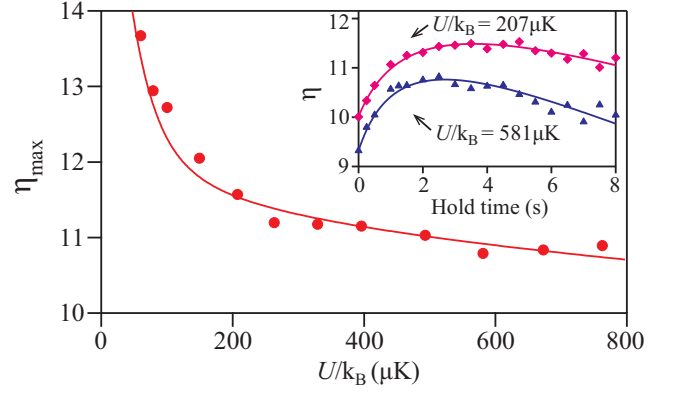


FIG. 4. (color online) η_{max} as a function of the ODT depth U , when atoms are held at a fixed U for 8 s. The solid line is a fit based on Eqs. (1-2) (see text). Inset: the time evolution of η at two typical ODT depths. Solid lines are fits based on the same model applied in the main figure (see text).

The value of η in many publications on optical productions of BECs was held constant with $\Delta\eta = 0$ [6, 7, 11, 12, 14, 15, 17]. Our data in Fig. 3, however, shows that a constant η does not lead to better evaporation or a larger γ . The values of γ in this figure are extracted from 36 evaporation processes in which the forced evaporation speed and the hold time at U_{max} are changed independently, although they all start with the same initial number of cold atoms in the crossed ODT. $\Delta\eta = \eta_f - \eta_i$ is the change of η during forced evaporation, where η_i and η_f are the values of η at U_{max} (i.e., the beginning of forced evaporation), and at U_f , respectively. In order to avoid overestimating γ due to the Bose enhancement near the BEC transition temperature, we choose $U_f = k_B \times 30 \mu\text{K}$ where no BEC appears. We find that $\Delta\eta$ tends to be a non-negative value when the forced evaporation time is longer than 1 s (closed black squares in Fig. 3), which is a good indication of sufficient rethermalization. We also find that γ is too small to yield a BEC when $\Delta\eta < -2.5$.

We compare the evaporation efficiency at different values of η_i , as shown in the inset of Fig. 3. γ_{best} (the best achieved value of γ at a given η_i in our system) does not show a strong dependence on η_i if $8 < \eta_i < 10$, while γ_{best} sharply diminishes when η_i becomes too large or too small. In the inset of Fig. 3, the similar relationship between γ and η_i is also predicted by the solid (blue) line, which is a result based on Eq. (4) by ignoring k_1 and k_s and by applying a non-zero R (i.e. $R_{\text{gTb}} = 4000$ [4]). All of our data lie below the solid line in this figure, which may indicate that k_1 and k_s are larger than 0 and cannot be ignored. Therefore, based on Fig. 3, we need to choose a value between 8 and 10 for η_i and keep $\Delta\eta$ larger than -0.5 in order to optimize evaporation efficiency γ .

The maximum achievable value for η_i appears to be 10.8, as shown in the inset of Fig. 3. To understand this, we monitor the time evolution of η and find that η has a maximal value (η_{max}) at a given ODT depth U . The value of η_{max} decreases exponentially with U and η_{max} at

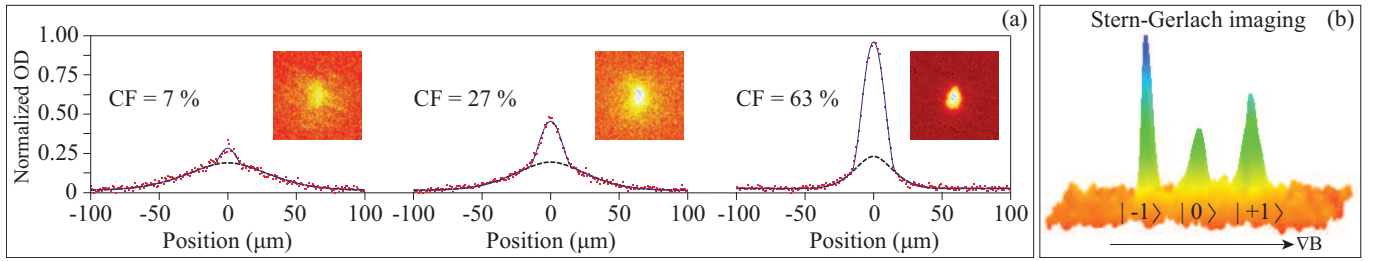


FIG. 5. (color online)(a). Absorption images taken after interrupting an optimized evaporation curve at various U followed by a 10 ms time-of-flight (see text). OD stands for the optical density. Dashed (black) lines and solid (blue) lines are fits to the column densities based on a Gaussian distribution and a bimodal distribution, respectively. $CF = \tilde{n}_c/(\tilde{n}_{th} + \tilde{n}_c)$, where \tilde{n}_{th} and \tilde{n}_c are column densities for the thermal cloud and the condensate, respectively. (b). Three spin components of a $F=1$ spinor BEC are spatially separated in a 3D Stern-Gerlach absorption image.

U_{max} is 10.8, which agrees well with our theoretical prediction (solid red line in Fig. 4). Therefore, if one wishes to keep η unchanged during forced evaporation, η must be limited to 10.8 even though η_{max} can be much higher at low ODT depths (e.g., $\eta_{max} > 13$ for $U/k_B < 100 \mu K$). This may be one reason why a constant η does not yield more efficient evaporative cooling. We also find that the time evolution of η at every U discussed in this paper can be well fit with our model. Two typical fitting curves are shown in the inset of Fig. 4.

A pure $F=1$ BEC of 1.2×10^5 sodium atoms at 50 nK is created from a 0.45 s free evaporation at U_{max} followed by a 5 s forced evaporation in which U is exponentially reduced. This evaporation curve provides two important parameters for efficient evaporative cooling: η_i is between 8 and 10, and the forced evaporation time is long enough for sufficient rethermalization but short enough to avoid excessive atom losses. Three time-of-flight absorption images in Fig. 5(a) show a typical change of the condensate fraction (CF) after interrupting the evaporation curve at various U . When an external magnetic field gradient is applied, three spin components in a $F=1$ BEC spatially

separate, as shown in Fig. 5(b). We also apply the above all-optical approach to evaporate atoms in a single-beam ODT. A similar result can also be achieved in the single-beam ODT as long as its $1/e^2$ beam waist is smaller than $16 \mu m$ to provide a high enough collision rate.

In conclusion, we have presented an optimal experimental scheme for an all-optical production of sodium spinor BECs. With this scheme, the number of atoms in a pure BEC is greatly boosted by a factor of 5 and $\gamma = 3.5$ is achieved in a simple setup that includes a single-beam ODT or a crossed ODT. We have showed an upper limit for γ at a given η , demonstrated that a constant η could not yield a larger γ , and discussed good agreements between our model and experimental data. This optimal scheme avoids technical challenges associated with some all-optical BEC approaches, and can be applied to other optically trappable atomic species and molecules [24].

We thank the Army Research Office, Oklahoma Center for the Advancement of Science & Technology, and Oak Ridge Associated Universities for financial support. M. Webb thanks the Niblack Research Scholar program. N. Jiang and H. Yang thank the National Basic Research Program of China.

-
- [1] K. B. Davis, M. -O. Mewes, M. R. Andrews, N. J. van Druten, D. S. Durfee, D. M. Kurn, and W. Ketterle, Phys. Rev. Lett. **75**, 3969 (1995).
 - [2] M. H. Anderson, J. R. Ensher, M. R. Matthews, C. E. Wieman, and E. A. Cornell, Science **269**, 198 (1995).
 - [3] C. C. Bradley, C. A. Sackett, J. J. Tollett, and R. G. Hulet, Phys. Rev. Lett. **75**, 1687 (1995).
 - [4] W. Ketterle and N. J. van Druten, Advances In Atomic, Molecular, and Optical Physics **37**, 181 (1996).
 - [5] Y.-J. Lin, A. R. Perry, R. L. Compton, I. B. Spielman, and J. V. Porto, Phys. Rev. A **79**, 063631 (2009).
 - [6] M. D. Barrett, J. A. Sauer, and M. S. Chapman, Phys. Rev. Lett. **87**, 010404 (2001).
 - [7] R. Dumke, M. Johanning, E. Gomez, J. D. Weinstein, K. M. Jones, and P. D. Lett, New Journal of Physics **8**, 64 (2006).
 - [8] T. Weber, J. Herbig, M. Mark, H.-C. Nägerl, and R. Grimm, Science **299**, 232 (2003).
 - [9] C. S. Adams, H. J. Lee, N. Davidson, M. Kasevich, and S. Chu, Phys. Rev. Lett. **74**, 3577 (1995).
 - [10] K. J. Arnold and M. D. Barrett, Optics Communications **284**, 3288 (2011).
 - [11] T. Kinoshita, T. Wenger, and D. S. Weiss, Phys. Rev. A **71**, 011602 (2005).
 - [12] J.-F. Clément, J.-P. Brantut, M. Robert-de-Saint-Vincent, R. A. Nyman, A. Aspect, T. Bourdel, and P. Bouyer, Phys. Rev. A **79**, 061406 (2009).
 - [13] Y. Takasu, K. Maki, K. Komori, T. Takano, K. Honda, M. Kumakura, T. Yabuzaki, and Y. Takahashi, Phys. Rev. Lett. **91**, 040404 (2003).
 - [14] A. J. Olson, R. J. Niffenegger, and Y. P. Chen, Phys. Rev. A **87**, 053613 (2013).
 - [15] S. R. Granade, M. E. Gehm, K. M. O'Hara, and J. E. Thomas, Phys. Rev. Lett. **88**, 120405 (2002).

- [16] J. Stenger, S. Inouye, D. M. Stamper-Kurn, H.-J. Miesner, A. P. Chikkatur, and W. Ketterle, *Nature* **396**, 345 (1998).
- [17] C.-L. Hung, X. Zhang, N. Gemelke, and C. Chin, *Phys. Rev. A* **78**, 011604 (2008).
- [18] D. M. Stamper-Kurn, M. Ueda, arXiv:1205.1888 (2012).
- [19] L. Zhao, J. Jiang, J. Austin, M. Webb, Y. Pu, and Y. Liu, to be published (2013).
- [20] The first polarization gradient cooling step compresses the MOT for 20 ms by increasing the power of each cooling beam to 12 mW while changing δ to -15 MHz. In this step, the power of each MOT repumping beam is also drastically reduced to $45 \mu\text{W}$. Then during a 5 ms pre-molasses step, every cooling beam is further red detuned in addition to its power being increased to 16 mW. This is followed by a 18 ms optical molasses, in which a cooling beam is detuned to $\delta = -45$ MHz and its power linearly drops to 8 mW. The magnetic field gradient is also reduced to 3 G/cm over the 18 ms.
- [21] K. M. O'Hara, M. E. Gehm, S. R. Granade, and J. E. Thomas, *Phys. Rev. A* **64**, 051403 (2001).
- [22] O. J. Luiten, M. W. Reynolds, and J. T. M. Walraven, *Phys. Rev. A* **53**, 381 (1996).
- [23] M. Yan, R. Chakraborty, A. Mazurenko, P. G. Mickelson, Y. N. Martinez de Escobar, B. J. DeSalvo, and T. C. Killian, *Phys. Rev. A* **83**, 032705 (2011).
- [24] Upon completion of this work, we have recently become aware of Ref [25] and their ODT ramp sequence which linearly ramps ODTs from $U_{\text{max}}/3$ to U_{max} in $t_{\text{ramp}}=2$ s. We find that the number of atoms in a pure BEC exponentially decreases with t_{ramp} when $t_{\text{ramp}} > 0.01$ s in our system. The optimal sequence explained in our paper yields a pure BEC of at least twice the number of atoms than that from a sequence with $t_{\text{ramp}}=2$ s for our apparatus.
- [25] D. Jacob, E. Mimoun, L. D. Sarlo, M. Weitz, J. Dalibard, and F. Gerbier, *New Journal of Physics* **13**, 065022 (2011).